Macromolecules **1998,** *31,* 1398−1405

Cholesteric Pitch of Lyotropic Polymer Liquid Crystals

Takahiro Sato,* Jun Nakamura,[†] and Akio Teramoto[‡]

Department of Macromolecular Science, Osaka University, Machikaneyama-cho 1-1,
Toyonaka, Osaka 560-0043, Japan

Mark M. Green

Department of Chemistry and Herman F. Mark Polymer Research Institute, Polytechnic University,
Six Metrotech Center, Brooklyn, New York 11201

Received July 1, 1997; Revised Manuscript Received November 4, 1997

ABSTRACT: The cholesteric pitch P of semiflexible helical polymer solutions was formulated using a threaded equivalent freely jointed chain model. The theory was favorably compared with experimental results of P for cholesteric solutions of the three helical polymers schizophyllan (a triple-helical polysaccharide), poly(γ-benzyl L-glutamate), and poly((R)-2,6-dimethylheptyl isocyanate), and two chiral interaction parameters characterizing the chiral hard-core repulsion and the soft dispersion force were determined from this comparison. However, the same theory failed to describe the polymer concentration dependence of P for cholesteric solutions of (acetoxypropyl)cellulose in a very concentrated region.

1. Introduction

The structure of cholesteric liquid crystals is characterized by the cholesteric pitch P or the cholesteric wavenumber q_c ($\equiv 2\pi/P$). Robinson[1,2] pioneered the study of the cholesteric pitch of lyotropic polymer liquid crystals. He observed that P for liquid-crystalline solutions of α-helical poly(γ-benzyl L-glutamate) (PBLG) depends strongly on the polymer concentration and the solvent but little on the polymer molecular weight. After his work, the cholesteric pitch was studied for various stiff or semiflexible polymer solutions.[3−12]

Theoretically, many workers calculated P for polymer cholesterics using the straight-rod model.[13−22] In those theories are discussed two origins inducing the cholesteric helical structure: the hard-core repulsion and the chiral dispersion force between threaded or helicoidal rods. Those theories, however, predict a strong molecular-weight dependence of P, which was inconsistent with Robinson's experimental results.[1,2]

Recently, Sato and Teramoto[23] formulated the free energy of semiflexible polymer solutions in a distorted nematic state to calculate the Frank elastic constants K_i for the splay ($i = 1$), twist ($i = 2$), and bend ($i = 3$) distortions. They used the *equivalent freely jointed chain* (EFJC) model to incorporate effects of the polymer chain flexibility into K_i and showed that the flexibility is essentially important in K_i even for polymer chains taking nearly rodlike conformations (or with a small Kuhn segment number N). Their theory was favorably compared with experimental results for K_2 and K_3 of PBLG solutions reported by Meyer and co-workers.[24,25]

The above theory indicates that the polymer chain flexibility has an important role also in the cholesteric pitch, which was not considered in the previous theories for straight rods. Osipov et al.,[20,26] Odijk,[27] and Pelcovits[45] presented expressions of P for semiflexible polymer solutions in the coil limit. However, their results cannot be applied to less flexible polymer chains with small N, whereas most of the cholesteric pitch experiments were made for such semiflexible polymer samples.

In the present study, we have derived an expression of P for semiflexible polymer solutions by extending the previous theory.[23] We have used the EFJC with a thread as the cholesteric polymer model and taken into account the twisting forces induced by both hard-core repulsion and the chiral dispersion force. In contrast with previous workers' results, the present expression of P is valid for polymer chains with arbitrary flexibility.

The derived expression of P has been compared with experimental data for cholesteric solutions of the helical polymers PBLG,[1,2,28] poly((R)-2,6-dimethylheptyl isocyanate) (PNIC),[12] and schizophyllan (a triple-helical polysaccharide). The cholesteric pitch for aqueous schizophyllan solutions has been newly measured in this study and added to literature data[29] to compare with the theory. From the comparison between theory and experiment, we can estimate interaction parameters characterizing the chiral hard-core repulsion and the dispersion force between polymer chains.

2. Formulation

A. Polymer Model and Chiral Interactions. Most lyotropic liquid-crystalline polymers are represented by the wormlike cylinder (WC) model, which is characterized by the contour length L, the hard-core diameter d, and the persistence length q. However, its chain statistics are hard to deal with in a inhomogeneous liquid-crystal field. Sato and Teramoto[23] replaced the WC by the equivalent freely jointed chain (EFJC) to calculate the Frank elastic constants. This EFJC model is defined as a freely jointed chain with the orientational order parameter S the same as that of the WC with the same L and d in a liquid-crystalline solution. This condition relates the segment length κ

[†] Present address: Sharp Corporation, 2613-1 Ichinomoto-cho, Tenri, Nara 632, Japan.

[‡] Present address: Department of Chemistry, Faculty of Science and Engineering, Ritsumeikan University, Noji-higashi, Kusatsu, Shiga 525-77, Japan.

S0024-9297(97)00968-6 CCC: $15.00

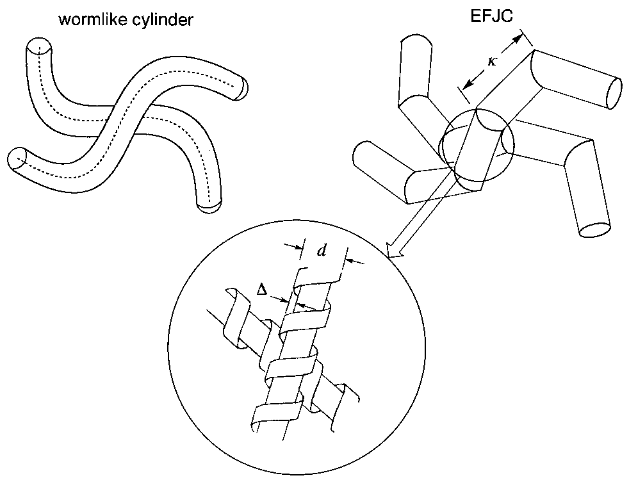

Figure 1. Threaded effective freely jointed chain (EFJC) model.

of the EFJC to q of the WC by

$$\kappa = 2q\left\{\frac{1}{N} + \frac{1 + \frac{1}{2}\tanh\left[\frac{2}{5}N(\alpha - 1)\right]}{3[\alpha^{-1} - \pi \exp(-\alpha)]}\right\}^{-1} \tag{1}$$

where N ($\equiv L/2q$) is the number of Kuhn's statistical segments and α is the variational parameter which is included in the Onsager trial function[30] for the average orientational distribution function $f(\mathbf{a})$ with respect to the tangent vector **a** of the WC, given by

$$f(\mathbf{a}) = (\alpha/4\pi \sinh \alpha) \cosh(\alpha\mathbf{a}\cdot\mathbf{n})$$

(**n**: the director). The parameter α represents the degree of orientation of **a** in the nematic solution, being calculated from the free energy minimization condition mentioned below. The segment length κ depends on the polymer concentration and molecular weight through α and N. In the rod limit ($N \rightarrow 0$), κ is equal to the contour length L. On the other hand, in the coil limit ($N \rightarrow \infty$), $\kappa = 6q(\alpha^{-1} - \pi e^{-\alpha})$.

Straley[13] proposed, in his theory of polymer cholesterics, a threaded rod model for helical polymers forming cholesteric phases in concentrated solution. Similarly, we here represent chiral polymers by a threaded EFJC model, as shown schematically in Figure 1. The thread height is denoted by Δ and taken as a parameter characterizing the chiral repulsive interaction between polymer chains.

Osipov[17,19,20] obtained the dispersion energy between two chiral macromolecules by extending the McLachlan theory[31,32] for the dispersion force between macroscopic bodies. His final result for the chiral part w_C of the dispersion energy is given by

$$w_C = -J^*\int_{-L/2}^{L/2} \mathrm{d}s\int_{-L/2}^{L/2} \mathrm{d}s'\frac{1}{x^7}[(\mathbf{a}\cdot\mathbf{a}') - 6(\mathbf{a}\cdot\mathbf{e})(\mathbf{a}'\cdot\mathbf{e})](\mathbf{a} \times \mathbf{a}'\cdot\mathbf{e}) \tag{2}$$

where **a** and **a**′ are the tangent vectors to the contour points s and s' on the centroids of the two chains, x is the distance between the points s and s', and **e** is a unit vector directed from s to s'. The coupling constant J^* is defined by

$$J^* \equiv (6\hbar/\pi) \int_0^{\infty} \mathrm{d}\omega\Delta\alpha^*(\omega)\, \Delta g^*(\omega)/\epsilon_m^{\ 2}(\omega) \tag{3}$$

where $\Delta\alpha^*(\omega)$ and $\Delta g^*(\omega)$ are the frequency (ω)-dependent anisotropies of the molecular polarizability and of the gyration tensor, respectively, and $\epsilon_m(\omega)$ is the solvent dielectric permittivity ($\hbar$: the Planck constant divided by 2π). The parameter J^* is a pseudoscalar quantity, which changes sign when the handedness of the molecule is changed. It is not easy to estimate J^* with eq 3 because the data for $\Delta\alpha^*(\omega)$ and $\Delta g^*(\omega)$ are not readily available. In what follows, we regard J^* as an adjustable parameter characterizing the chiral dispersion interaction between polymer chains.

After performing the integration over the chain contours s and s' in eq 2 under the condition of the crossed configuration (i.e., where both the closest contour points $\tilde{s}$ and $\tilde{s}'$ on the centroids of the two chains are not the chain end point),[33] we have

$$w_C = \frac{7\pi J^*}{24|\mathbf{p}|^6|\tilde{\mathbf{a}} \times \tilde{\mathbf{a}}'|}(\tilde{\mathbf{a}}\cdot\tilde{\mathbf{a}}')(\tilde{\mathbf{a}} \times \tilde{\mathbf{a}}'\cdot\mathbf{p}) \tag{4}$$

where **p** is the vector connecting the closest contour point $\tilde{s}$ to $\tilde{s}'$ and $\tilde{\mathbf{a}}$ and $\tilde{\mathbf{a}}'$ are the tangent vectors to the closest contour points $\tilde{s}$ and $\tilde{s}'$; **p** is parallel or antiparallel to the vector $\tilde{\mathbf{a}} \times \tilde{\mathbf{a}}'$. This equation holds when the persistence length (and also the contour length) is much longer than the range of the dispersion interaction, a condition probably met in most cases. In the following theoretical development, we neglect the interaction at the noncrossed configuration, which may be justified for polymers of practical interest.

B. Cholesteric Pitch. In a twisted nematic state, the Helmholtz free energy density F of a semiflexible polymer solution is written as[23]

$$F = F_N - K_t q_2 + \frac{1}{2}K_2 q_2^{\ 2} \tag{5}$$

where q_2 is the wavenumber of the twist distortion, F_N is the free energy density in the undistorted nematic state, K_t is the twisting force constant, and K_2 is the Frank elastic constant for the twist distortion.

Sato and Teramoto[23] calculated F_N and K_2 using the EFJC model. The free energy density F_N is given in the appendix of their paper. The variational parameter α appearing in eq 1 is determined from the minimization condition of F_N, which reads[23]

$$\frac{\mathrm{d}\sigma_{WC}}{\mathrm{d}\alpha} + \frac{\pi}{4}(L - d)^2 dc' H_A(\phi)\frac{\mathrm{d}\rho}{\mathrm{d}\alpha} = 0 \tag{6}$$

where c' is the number concentration of the polymer chain, σ_{WC} and ρ are the conformational entropy loss (of the WC) and the reduction of the intermolecular excluded volume, respectively, by the chain orientation, both of which are known functions of α, and $H_A(\phi)$ is a function of the polymer volume fraction ϕ defined by

$$H_A(\phi) = \frac{1}{1 - \phi}\left[1 + \frac{2(X' + 1)\phi}{(3X' + 2)(1 - \phi)}\right] \tag{7}$$

with $X' \equiv L/d - 1$. The elastic constant K_2 is calculated to be

$$K_2 = \frac{1}{12}\kappa^4 dc_\kappa'^{\,2} k_B T H_A(\phi)\, I_2(S) \tag{8}$$

where c'_κ is the number concentration of EFJC segments, k_BT is the Boltzmann constant multiplied by the absolute temperature, and $I_2(S)$ is a function of the orientational order parameter S, defined by[34]

$$I_2(\phi) = \frac{7}{16}\left[\frac{\pi}{3}(1 - S)\right]^{1/2}(0.1138 - 0.5579S + 1.9484S^2 - 0.5043S^3) \quad (9)$$

In eqs 6 and 8, soft dispersion force terms have been neglected, since these are not usually important in lyotropic polymer liquid crystals consisting of a semiflexible polymer and a good solvent. Equation 9 was obtained by using the Onsager trial function as $f(\mathbf{a})$, and the order parameter S is given by

$$S = 1 - \frac{3}{\alpha}\coth\alpha + \frac{3}{\alpha^2} \quad (10)$$

with α determined by eq 6.

The twisting force constant K_t takes a nonzero value only for chiral polymer systems. Using the threaded EFJC model with the chiral interaction described above, the calculation of K_t is carried out in the Appendix with the result given by eq A9. The twisting force induced by the hard-core repulsion does not necessarily overwhelm that induced by the chiral dispersion force, unlike in the case of K_2. Therefore, the latter contribution to K_t is kept in eq A9.

From the minimization condition of the free energy, eq 5, the cholesteric pitch P or the cholesteric wavenumber q_c can be calculated by

$$\frac{2\pi}{P} \equiv q_c = \frac{K_t}{K_2} \quad (11)$$

Inserting eqs 8 and A9 into eq 11, we obtain the result

$$q_c = \frac{K_t}{K_2} = \frac{6S^2}{\kappa^2 I_2(S)}\left[\lambda\Delta + \frac{\delta^*}{H_A(\phi)}\right] \quad (12)$$

where λ and δ^* are defined by eqs A6 and A8, respectively. Since λ and δ^* are pseudoscalar parameters, we have to define their signs. In what follows, we assign positive λ and δ^* for the right-handed twisting forces. Therefore, a positive (negative) q_c indicates a right-handed (left-handed) cholesteric helical structure. This agrees with the conventional definition of the sign of q_c. In ref 12, q_c was divided into the entropic term (S_q) and the enthalpic term (H_q/T), which correspond to the first and second terms on the right-hand side of eq 12, respectively.

3. Experimental Section

Sonicated schizophyllan samples supplied by Taito Co. and stocked in our laboratory in Osaka were combined and repeatedly fractionated by fractional precipitation with water as the solvent and acetone as the precipitant. Three fractionated samples S21, S17, and S12 were used for the cholesteric pitch measurements. The intrinsic viscosities [η] for those samples in 25 °C water were determined on conventional Ubbelohde-type capillary viscometers, and viscosity-average molecular weights (M_v) were evaluated from the [η] data using the [η]−molecular weight relation established by Yanaki et al.[35] The results for [η] and M_v are listed in Table 1.

Table 1. Molecular Characterization of Schizophyllan Samples Used

sample	$[\eta]/10^2$ cm^3 g^{-1}	$M_v/10^4$	L^a/nm	N^a
S21	1.50	20.8	96.7	0.242
S17	1.06	17.0	76.1	0.198
S12	0.56	11.6	54.0	0.135

[a] Calculated from M_v with the wormlike chain parameters listed in Table 2.

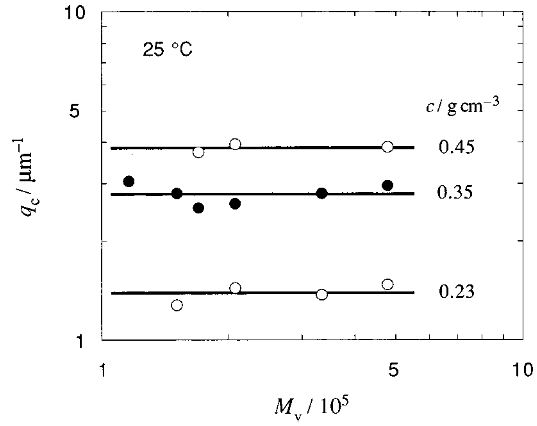

Figure 2. Plots of q_c against the viscosity-average molecular weight M_v for aqueous schizophyllan solutions with different polymer mass concentrations c at 25 °C. Data at $M_v/10^4$ = 15.2, 32.0, and 42.0 are taken from ref 29.

Cholesteric solutions of the above schizophyllan samples were prepared by mixing the samples with pure water and stirring vigorously for 2−3 days. Each solution was transferred into a drum-shaped cell with a 1-mm thickness, and the neck of the cell was sealed with an adhesive. Cholesteric pitch measurements were made at 25 °C by the laser diffraction method. The detailed procedure of this method was described elsewhere.[5,12] The cholesteric pitch P measured was transformed into the cholesteric wavenumber q_c using eq 11.

4. Results

Figure 2 plots q_c against the viscosity-average molecular weight M_v for aqueous schizophyllan solutions with different polymer mass concentrations c at 25 °C. The data points at M_v = 42.0 × 10^4, 32.0 × 10^4, and 15.2 × 10^4 are the results reported in ref 29. It can be seen that q_c is essentially independent of M_v at all the concentrations examined. The molecular-weight independence of q_c or P was observed also for dioxane solutions of poly(γ-benzyl L-glutamate) (PBLG),[1] except in the vicinity of the isotropic−cholesteric phase boundary concentration.[11]

Figure 3 shows the concentration dependence of q_c for schizophyllan solutions at 25 °C. In the double-logarithmic plot, the data points follow a curve concave upward, indicating that the concentration dependence of q_c (or P) is not described by a simple power law. The slope of the curve in the low-concentration region is 1.8. Robinson et al. reported a c^2 dependence of q_c for the PBLG−dioxane system, while Gray et al.[6] obtained a c^3 dependence of q_c for the (acetoxypropyl)cellulose (APC)−acetone system. The concentration dependence of q_c for aqueous schizophyllan resembles that of the PBLG solution.

5. Comparison between Theory and Experiment

Many cholesteric pitch measurements have been carried out for various helical polymer solution systems.

Table 2. Molecular Parameters of Various Helical Polymers

polymer	solvent	M_L/nm^{-1}	q/nm	d/nm	v_{sp}/cm^3 g^{-1}	ref
schizophyllan	water (25 °C)	2150	200	1.75		35, 40
PBLG[a]	DMF[d] (25 °C)	1450	150	1.42		36, 37, 40
PNIC[b]	*n*-hexane (25 °C)	970	76	1.43	1.00[f]	38
APC[c]	DMP[e] (25 °C)	821	5.9	1.2	0.825[g]	6, 39

[a] Poly(γ-benzyl L-glutamate). [b] Poly((*R*)-2,6-dimethylheptyl isocyanate). [c] (Acetoxypropyl)cellulose. [d] Dimethylformamide. [e] Dimethylphthalate. [f] Measured by Miss I. Terakawa at Osaka University. [g] In 25 °C acetone.

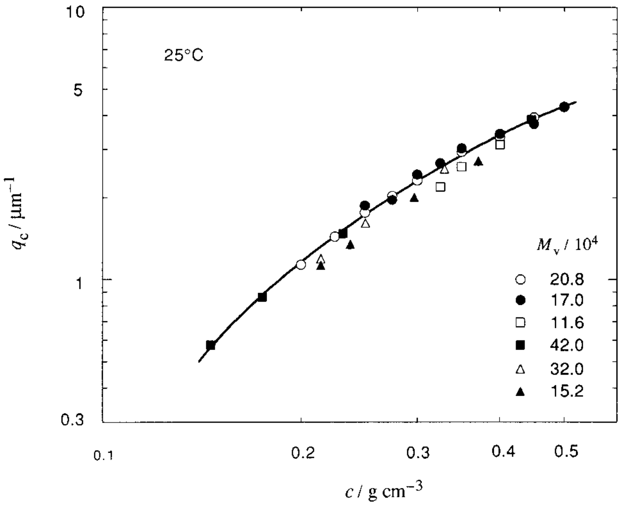

Figure 3. Concentration dependence of q_c for aqueous schizophyllan solutions with different molecular weights at 25 °C. Data for $M_v/10^4$ = 15.2, 32.0, and 42.0 are taken from ref 29.

In this section, we compare those pitch data as well as the data obtained in this study (cf. Section 4) with the theory (eq 12) formulated in Section 2. Here we focus our attention on the polymer concentration dependence of the cholesteric pitch *P*. Although the temperature dependence of *P* is also an interesting problem,[10,12] we do not analyze it in the present study.

To calculate *P* or q_c from eq 12, we need the wormlike cylinder parameters, the molar mass per unit contour length M_L, the persistence length *q*, and the hard-core diameter *d* of the polymer forming the cholesteric liquid crystal. The contour length *L* of the polymer is calculated from M_L and the molecular weight *M* of the polymer from $L = M/M_L$. The values of M_L and *q* for helical polymers examined in this section were previously estimated by established methods of dilute solution studies.[35-39] The results are listed in Table 2. The wormlike chain parameters for poly((*R*)-2,6-dimethylheptyl isocyanate) (PNIC) and (acetoxypropyl)cellulose (APC) were estimated in *n*-hexane and dimethyl phthalate, respectively, both of which are different from the solvents used for the cholesteric pitch measurements (see below). In the following, however, we neglect the difference in these solvent conditions.

The values of *d* for schizophyllan and PBLG were recently determined by analyzing the data of the second virial coefficient and osmotic pressure (or osmotic compressibility) of isotropic solutions.[40] The results are listed in the fourth column of Table 2. Since there are no such data for PNIC nor APC, the values of *d* for these polymers were estimated from the partial specific volume v_{sp} using the relation $d = (4v_{sp}M_L/\pi N_A)^{0.5}$. For schizophyllan and PBLG, *d* estimated from v_{sp} was a good approximation to the result listed in Table 2.[40]

Equation 12 includes also two chiral interaction parameters, the thread height Δ and the strength of the chiral dispersion force δ^*. These parameters may be determined from the cholesteric pitch data as follows. Equation 12 can be rewritten as

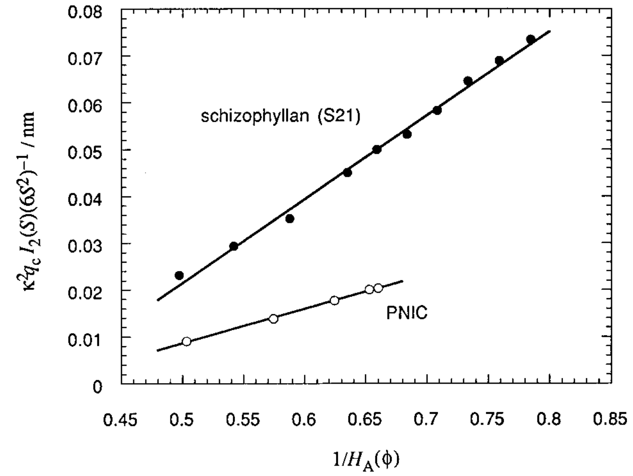

Figure 4. Plots of $q_c\kappa^2 I_2(S)/6S$ against $H_A(\phi)^{-1}$ for cholesteric solutions of the schizophyllan sample S21 and of a poly((*R*)-2,6-dimethylheptyl isocyanate) (PNIC) sample, from which the chiral interaction parameters $\lambda\Delta$ and δ^* are determined according to eq 13. The q_c data for PNIC solutions are taken from ref 12.[46]

$$\frac{q_c\kappa^2 I_2(S)}{6S^2} = \lambda\Delta + \frac{\delta^*}{H_A(\phi)} \tag{13}$$

The quantity on the left-hand side can be calculated with the experimental q_c as well as the theoretical κ, $I_2(S)$, and *S* evaluated by eqs 1, 9, and 10, respectively, with the molecular parameters listed in Table 2. The variational parameter α in those equations is determined by eq 6. On the other hand, $H_A(\phi)$ on the right-hand side can be calculated from eq 7 with the same molecular parameters and experimental concentration. Then $q_c\kappa^2 I_2(S)/6S$ is plotted against $H_A(\phi)^{-1}$, and if the plot is followed by a straight line, $\lambda\Delta$ and δ^* are determined from the intercept and slope of the line, respectively.

Figure 4 shows the plot of $q_c\kappa^2 I_2(S)/6S$ against $1/H_A(\phi)$ for aqueous solutions of the schizophyllan sample S21 ($M_v = 20.8 \times 10^4$) by filled circles; the data of q_c were taken from Figure 3. By least-squares fitting (the line shown in the figure), we determined $\lambda\Delta$ and δ^* to be -0.068 and 0.18 nm, respectively. Applying the same procedure to the other schizophyllan samples shown in Figure 3 (except for the sample with $M_v = 11.6 \times 10^4$), we obtained $\lambda\Delta$ and δ^* in the ranges indicated in Table 3. The signs of $\lambda\Delta$ and δ^* indicate that the twisting forces induced by the chiral hard-core and dispersion interactions are left-handed and right-handed, respectively. The chiral dispersion interaction is predominant in the twisting force for schizophyllan at room temperature.

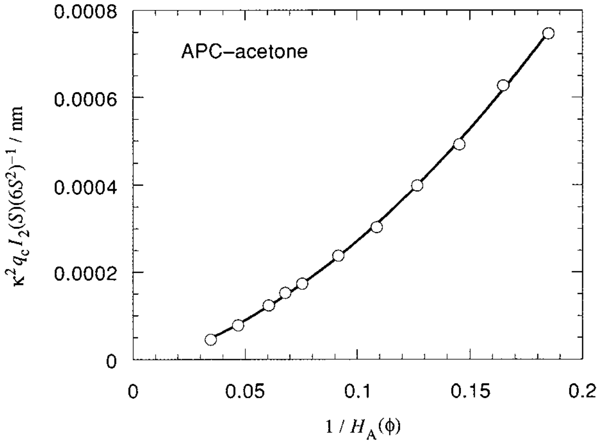

Figure 5. Plots of $q_c\kappa^2 I_2(S)/6S$ against $H_A(\phi)^{-1}$ for acetone solutions of (acetoxypropyl)cellulose (APC). The q_c data are taken from ref 6.

Table 3. Chiral Interaction Parameters of Helical Polymers Determined from Cholesteric Pitch Data

polymer	solvent	$\lambda\Delta$/nm	δ^*/nm
schizophyllan	water (25 °C)	−0.063 ± 0.008	0.17 ± 0.02
PBLG	dioxane (22, 25 °C)	−0.0051 ± 0.0025	0.017 ± 0.005
PNIC	toluene (43.7 °C)	−0.028	0.073_5

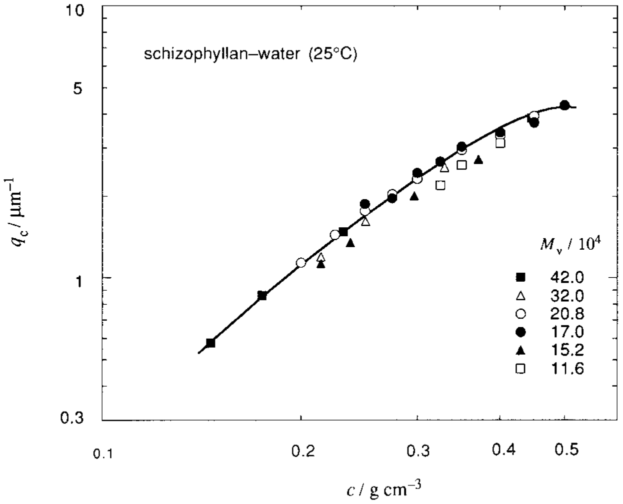

Figure 6. Comparison between theory and experiment for q_c for aqueous schizophyllan solutions. The theoretical values are calculated with eq 12 with $\lambda\Delta = -0.0581$ nm and $\delta^* = 0.162$ nm.

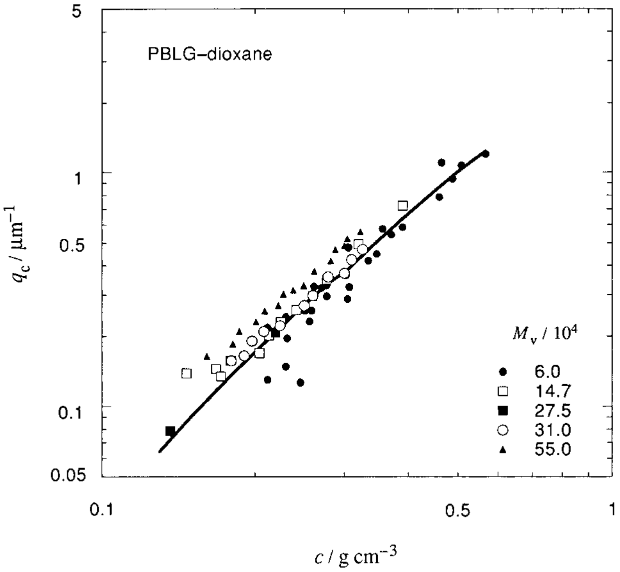

Figure 7. Comparison between theory and experiment for q_c for 1,4-dioxane solutions of poly(γ-benzyl L-glutamate) (PBLG). Data for $M_v/10^4$ = 6.0, 14.7, and 27.5 (at 22 °C) are taken from ref 1; data for $M_v/10^4$ = 31.0 and 55.0 (at 25 °C) are taken from ref 28; theoretical values are calculated with eq 12 with $\lambda\Delta = -0.00263$ nm and $\delta^* = 0.0127$ nm.

In Figure 4, the same plot is shown also for toluene solutions of PNIC at 43.7 °C by unfilled circles. The q_c data were taken from ref 12[46] and the molecular parameters of PNIC in toluene were approximated by those in *n*-hexane. This may be a plausible approximation, because the wormlike chain parameters of poly(*n*-hexyl isocyanate) are nearly the same in *n*-hexane and in toluene.[42,43] The results of $\lambda\Delta$ and δ^* obtained by least-squares fitting are −0.028 and 0.073_5 nm, respectively. For this polymer, the twisting forces induced by the chiral hard-core and dispersion interactions are also left-handed and right-handed, respectively,[41] and the chiral dispersion interaction is predominant in the cholesteric formation at room temperature.

The same procedure was applied to obtain the chiral interaction parameters for PBLG in 1,4-dioxane by using literature data[1,28] for the cholesteric pitch for three different molecular-weight samples and the molecular parameters listed in Table 2. For both schizophyllan and PBLG, the values of $\lambda\Delta$ and δ^* varied somewhat on the samples, and their ranges are shown in Table 3. It is seen in this table that the magnitudes of the chiral interaction parameters for PBLG are considerably smaller than those for schizophyllan and PNIC.

In Figure 5, we compare Gray et al.'s pitch data[6] for acetone solutions of (acetoxypropyl)cellulose (APC) with our theory, where the wormlike chain parameters in dimethyl phthalate given in Table 2 are used instead of those in acetone. It is clearly seen that eq 12 with constant values of $\lambda\Delta$ and δ^* fails to describe the concentration dependence of q_c for this system in contrast to the case for the above three helical polymer systems. The following explanations may be in order to reconcile this failure.

(1) The failure is characteristic of this system and does not represent the general behavior.

(2) The concentration range is much higher for the APC−acetone system (the weight fraction 0.7−0.9) compared with the other systems studied. At such high concentrations, some approximations used to derive K_2 and K_t become poor: for example, the neglect of higher perturbation terms with respect to w_C in eq A2 or an approximation to the direct correlation function used in the previous formulation[23] of the free energy functional.

(3) The side-chain and/or main-chain conformations may change with the polymer concentration *c*, causing the parameters $\lambda\Delta$ and δ^* to depend on *c*, although there is no evidence to support this.

Now, we can directly compare the theoretical and experimental q_c values for schizophyllan, PBLG, and PNIC solutions using the $\lambda\Delta$ and δ^* values determined. Figures 6 and 7 show the concentration dependence of q_c for schizophyllan and PBLG solutions. The solid curves in the figures indicate theoretical values calculated with eq 12 with $\lambda\Delta$ and δ^* chosen within the ranges shown in Table 3 so as to give the closest

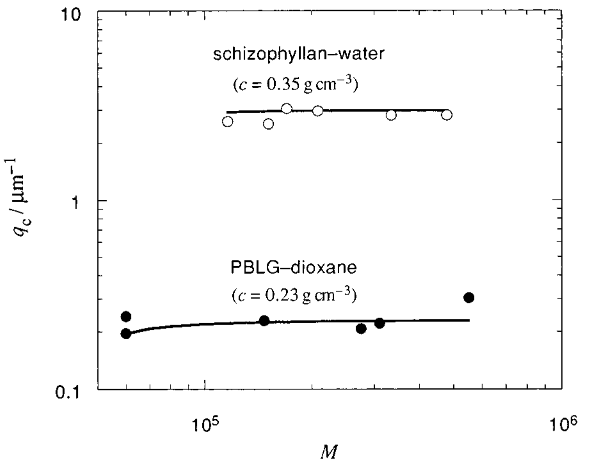

Figure 8. Comparison between theory and experiment of the molecular weight dependence of q_c for schizophyllan and poly(γ-benzyl L-glutamate) solutions.

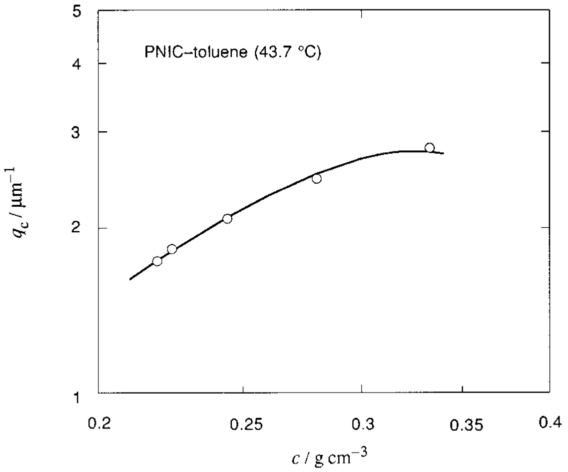

Figure 9. Comparison between theory and experiment for q_c for toluene solutions of poly((R)-2,6-dimethylheptyl isocyanate) (PNIC). Data are taken from ref 12;[46] theoretical values are calculated with $\lambda\Delta = -0.028$ nm and $\delta^* = 0.0735$ nm.

agreement between experiment and theory. The theoretical curves were virtually independent of the polymer molecular weight within the molecular weight and concentration ranges experimentally studied, as demonstrated in Figure 8 (the solid curves), which agrees with experimental results for both schizophyllan and PBLG.[44]

Figure 9 compares experimental results of PNIC solutions with the theory in the plot of q_c versus c, where the theoretical values (the solid curve) were calculated by using the values of $\lambda\Delta$ and δ^* listed in Table 3. The agreement between theory and experiment is also good for this system.

It should be noted that the value of q_c calculated from eq 12 is very sensitive to the values of $\lambda\Delta$ and δ^*, especially at high c, because q_c results from the subtraction of large numbers corresponding to the hard-core repulsion and dispersion force terms. Therefore, the least-squares fit in the plot of $q_c\kappa^2 I_2(S)/6S$ versus $1/H_A(\phi)$ does not necessarily give $\lambda\Delta$ and δ^*, which lead to the best fit in the plot of q_c versus c over the whole concentration range. For example, the values of $\lambda\Delta$ and δ^* estimated from the least-squares *linear* fit in the plot of $q_c\kappa^2 I_2(S)/6S$ versus $1/H_A(\phi)$ shown in Figure 5, for the APC–acetone system, provided theoretical q_c values which deviate greatly from the experimental data at high c, although it is not shown here graphically.

6. Conclusions

The cholesteric pitch P or the cholesteric wavenumber q_c ($\equiv 2\pi/P$) for lyotropic liquid crystals of semiflexible helical polymers has been formulated using the threaded equivalent freely jointed chain model. For the model, the rod segment length κ can be calculated from wormlike cylinder parameters (cf. eq 1), and the chiral intermolecular interaction is characterized by the thread height Δ and the strength δ^* of a chiral dispersion force. The formulated P or q_c is expressed in terms of $\lambda\Delta$ (λ: a numerical constant of order of unity) and δ^* as well as the wormlike cylinder parameters (the contour length, the persistence length, and the hard-core diameter). The wormlike cylinder parameters can be determined from isotropic solution studies.

The theory formulated has been compared with pitch data of cholesteric solutions of four chiral stiff polymers, schizophyllan, poly(γ-benzyl L-glutamate) (PBLG), poly((R)-2,6-dimethylheptyl isocyanate) (PNIC), and (acetoxypropyl)cellulose (APC), obtained in this study or reported in the literature. The polymer concentration and molecular-weight dependences of P for schizophyllan and PBLG, as well as the polymer concentration dependence for PNIC, were successfully reproduced by the theory with the suitably chosen chiral interaction parameters $\lambda\Delta$ and δ^*. On the other hand, the concentration dependence of P for very concentrated solutions of APC could not be fitted by the present theory. The reason for this failure remains open to question. We now plan to study the cholesteric pitch of other cellulose derivatives to elucidate the reason.

Acknowledgment. We are indebted to Prof. G. Gottarelli at Università di Bologna and Dr. S. Itou at Aichi College of Technology for pointing out refs 49 and 11, respectively. This work was partially supported by a Grant-in-Aid for Scientific Research (No. 09650999) from the Ministry of Education, Science, Sports, and Culture of Japan. Work at Polytechnic University was supported by the Chemistry and Material Divisions of the National Science Foundation and by the Office of Naval Research.

Appendix. Calculation of K_t

Using the EFJC model, the twisting force constant K_t is written as[23]

$$K_t = \frac{1}{2} c_\kappa'^2 k_B T \int\int d\tilde{\mathbf{a}}\; d\tilde{\mathbf{a}}' |\tilde{\mathbf{a}} \times \tilde{\mathbf{a}}'| C_2 f(\tilde{a}_z) \tilde{a}'_x f'(\tilde{a}'_z) \qquad \text{(A1)}$$

with the derivative $f'(\tilde{a}_z') \equiv \mathrm{d}f(\tilde{a}_z')/\mathrm{d}\tilde{a}_z'$ and[34]

$$C_2 = \int_{-\kappa/2}^{\kappa/2} \mathrm{d}\tilde{s} \int_{-\kappa/2}^{\kappa/2} \mathrm{d}\tilde{s}' \int_{-\infty}^{\infty} \mathrm{d}p [H_A(\phi)\Phi_0 + \Phi^*{}_w](\mathbf{p}\cdot\mathbf{e}_y) \qquad \text{(A2)}$$

Here Φ_0 and $\Phi^*{}_w$ are the Mayer functions with respect to the hard-core potential and the chiral dispersion potential in the crossed configuration, $\tilde{s}$ and $\tilde{s}'$ are the closest contour points on the centroids of two interacting EFJCs, and $\tilde{\mathbf{a}}$ and $\tilde{\mathbf{a}}'$ are the unit vectors parallel to the closest EFJC segments which include the contour points $\tilde{s}$ and $\tilde{s}'$, respectively. Cartesian coordinates (x, y, z) have been chosen so the z- and y-axes are parallel to the director at the origin and the cholesteric axis, respectively, $\mathbf{e}_y$ is the unit vector in the y direction, and p is the closest distance between two polymer chains, and $\mathbf{p}$ is defined by

$$\mathbf{p} = p\frac{\tilde{\mathbf{a}} \times \tilde{\mathbf{a}}'}{|\tilde{\mathbf{a}} \times \tilde{\mathbf{a}}'|} \tag{A3}$$

In eq A2, the achiral dispersion potential has been omitted because it has no contribution to C_2, and higher order perturbation terms with respect to w_C have been neglected on the assumption that w_C is weak enough.

The Mayer functions Φ_0 and Φ^*_w for a threaded EFJC (cf. Figure 1) may be expressed by

$$\Phi_0 = \begin{cases} -1, & |s| \text{ and } |s'| < L_c/2,\ -d^* \le p \le d^{**} \\ 0, & \text{otherwise} \end{cases} \tag{A4a}$$

and

$$\Phi^*_w = \begin{cases} -w_C/k_BT, & |s| \text{ and } |s'| < L_c/2,\ p > -d^*,\ d^{**} < p \\ 0, & \text{otherwise} \end{cases} \tag{A4b}$$

where we have used the high-temperature approximation to Φ^*_w. The thickness parameters d^* and d^{**} may be expressed as

$$d^* = d + \frac{1}{2}c(\tilde{\mathbf{a}}\cdot\tilde{\mathbf{a}}')\Delta, \quad d^{**} = d - \frac{1}{2}c(\tilde{\mathbf{a}}\cdot\tilde{\mathbf{a}}')\Delta \tag{A5}$$

where d and Δ are defined in Figure 1 and $c(\tilde{\mathbf{a}}\cdot\tilde{\mathbf{a}}')$ is a function of $\tilde{\mathbf{a}}\cdot\tilde{\mathbf{a}}'$. The function $c(\mathbf{a}, \mathbf{a}')$ depends on $\tilde{\mathbf{a}}\cdot\tilde{\mathbf{a}}'$ in a complicated way, and its explicit formulation is difficult. Straley[13] just assumed

$$c(\tilde{\mathbf{a}}\cdot\tilde{\mathbf{a}}') = \lambda\tilde{\mathbf{a}}\cdot\tilde{\mathbf{a}}' \tag{A6}$$

with a constant λ of order of unity, and we use his $c(\tilde{\mathbf{a}}\cdot\tilde{\mathbf{a}}')$ in the following. The constant λ is a pseudoscalar; that is, it changes the sign when the handness of the molecule (or the threaded EFJC) is changed.

Using eqs A4–A6, we can calculate C_2 as

$$C_2 = \kappa^2 d[\lambda\Delta H_A(\phi) + \delta^*](\tilde{\mathbf{a}}\cdot\tilde{\mathbf{a}}')\frac{\tilde{\mathbf{a}} \times \tilde{\mathbf{a}}'\cdot\mathbf{e}_y}{|\tilde{\mathbf{a}} \times \tilde{\mathbf{a}}'|} \tag{A7}$$

with

$$\delta^* \equiv \frac{7\pi J^*}{36k_BTd^4} \tag{A8}$$

Inserting eq A7 into eq A1, we have

$$K_t = \frac{1}{2}k_BT\kappa^2 dc_\kappa'^2[\lambda\Delta H_A(\phi) + \delta^*]S^2 \tag{A9}$$

where S is the orientational order parameter.

References and Notes

(1) Robinson, C.; Ward, J. C.; Beevers, R. B. *Discuss. Faraday Soc.* **1958**, *25*, 29.
(2) Robinson, C. *Tetrahedron* **1961**, *13*, 219.
(3) Uematsu, Y.; Uematsu, I. In *Mesomorphic Order in Polymers*; ACS Symposium Series, No. 74; American Chemical Society: Washington, DC, 1978; Chapter 11.
(4) Senechal, E.; Maret, G.; Dransfeld, K. *Int. J. Biol. Macromol.* **1980**, *2*, 256.
(5) Van, K.; Norisuye, T.; Teramoto, A. *Mol. Cryst. Liq. Cryst.* **1981**, *78*, 123.
(6) Tseng, S.-L.; Valente, A.; Gray, D. G. *Macromolecules* **1981**, *14*, 715.
(7) Guo, J.-X.; Gray, D. G. *Macromolecules* **1989**, *22*, 2082.
(8) Maret, G.; Milas, M.; Rinaudo, M. *Polym. Bull.* **1981**, *4*, 291.
(9) Yanaki, T.; Norisuye, T.; Teramoto, A. *Polym. J.* **1984**, *16*, 165.
(10) Uematsu, I.; Uematsu, Y. *Adv. Polym. Sci.* **1984**, *59*, 37.
(11) Itou, S. *Mol. Cryst. Liq. Cryst.* **1989**, *172*, 201.
(12) Sato, T.; Sato, Y.; Umemura, Y.; Teramoto, A.; Nagamura, Y.; Wagner, J.; Weng, D.; Okamoto, Y.; Hatada, K.; Green, M. M. *Macromolecules* **1993**, *26*, 4551.
(13) Straley, J. P. *Phys. Rev. A* **1976**, *14*, 1835.
(14) Samulski, T. V.; Samulski, E. T. *J. Chem. Phys.* **1977**, *67*, 824.
(15) Kimura, H.; Hosino, M.; Nakano, H. *J. Phys. (Paris)* **1979**, *40*, *C3*, 174.
(16) Kimura, H.; Hosino, M.; Nakano, H. *J. Phys. Soc. Jpn.* **1982**, *51*, 1584.
(17) Osipov, M. A. *Chem. Phys.* **1985**, *96*, 259.
(18) Osipov, M. A. *Polym. Sci. U. S. S. R.* **1987**, *29*, 1761.
(19) Osipov, M. A. *Il. Nuovo Cimento D* **1988**, *10*, 1249.
(20) Osipov, M. A. In *Liquid Crystalline and Mesomorphic Polymers*; Shibaev, V. P., Lam, L., Eds.; Springer: Berlin & Heidelberg, 1994; Chapter 1.
(21) Varichon, L.; ten Bosch, A.; Sixou, P. *Liq. Cryst.* **1991**, *9*, 701.
(22) Varichon, L.; Ten Bosch, A. *Macromolecules* **1992**, *25*, 3812.
(23) Sato, T.; Teramoto, A. *Macromolecules* **1996**, *29*, 4107.
(24) Taratuta, V. G.; Lonberg, F.; Meyer, R. B. *Phys. Rev. A* **1988**, *37*, 1831.
(25) Lee, S.-D.; Meyer, R. B. *Phys. Rev. Lett.* **1988**, *61*, 2217.
(26) Osipov, M. A.; Semenov, A. N.; Khokhlov, A. R. *Khim. Fiz.* **1987**, *6*, 1312.
(27) Odijk, T. *J. Phys. Chem.* **1987**, *91*, 6060.
(28) DuPré, D. B.; Duke, R. W. *J. Chem. Phys.* **1975**, *63*, 143.
(29) Itou, T.; Van, K.; Teramoto, A. *J. Appl. Polym. Sci., Appl. Polym. Symp.* **1985**, *41*, 35.
(30) Onsager, L. *Ann. N. Y. Acad. Sci.* **1949**, *51*, 627.
(31) McLachlan, A. D. *Proc. R. Soc. London* **1963**, *A271*, 387.
(32) McLachlan, A. D. *Proc. R. Soc. London* **1963**, *A274*, 80.
(33) Sato, T.; Teramoto, A. *Physica* **1991**, *A176*, 72.
(34) In ref 23, eqs 4.6, 4.8, and 4.11 have errors. The sign of the right-hand side of those equations should be opposite, and the last term in the brackets on the right-hand side of eq 4.6 should be taken out.
(35) Yanaki, T.; Norisuye, T.; Fujita, H. *Macromolecules* **1980**, *13*, 1462.
(36) Brelsford, G. L.; Krigbaum, W. R. In *Liquid Crystallinity in Polymers*; Ciferri, A., Ed.; VCH Publishers: New York, 1991; Chapter 2.
(37) Itou, S.; Nishioka, N.; Norisuye, T.; Teramoto, A. *Macromolecules* **1981**, *14*, 904.
(38) Gu, H. Ph.D. Thesis, Osaka University, 1997.
(39) Laivins, G. V.; Gray, G. D. *Macromolecules* **1985**, *18*, 1746.
(40) Sato, T.; Jinbo, Y.; Teramoto, A. *Macromolecules* **1997**, *30*, 590.
(41) Now the corrected twisting force sense of the hard-core repulsion is inconsistent with Straley's screw model[12,13] for the left-handed helix of PNIC.[48] There are some other examples being inconsistent with Straley's model; see, for example, ref 49.
(42) Itou, T.; Chikiri, H.; Teramoto, A.; Aharoni, S. M. *Polym. J.* **1988**, *20*, 143.
(43) Norisuye, T.; Tsuboi, A.; Teramoto, A. *Polym. J.* **1996**, *28*, 357.
(44) The theory predicts a decrease of q_c with decreasing polymer molecular weight in the vicinity of the isotropic–cholesteric phase boundary. (The phase boundary concentration is 0.23 g/cm^3 at $M = 44\,000$ for the PBLG–dioxane system; cf. Figure 8.) This prediction also agrees with Itou's cholesteric pitch results[11] of the PBLG–dioxane system.
(45) Pelcovits, R. A. *Liq. Cryst.* **1996**, *21*, 361.
(46) Recently, Green et al.[47] observed a positive circular dichroism band at near 257 nm for a cholesteric toluene solution of PNIC in a planar texture, which indicates the right-handed cholesteric sense being opposite to that previously assigned from the ORD measurement.[12] A strongly *negative* optical activity of the PNIC helical molecule, which may predominantly contribute to ORD, may lead to the erroneous sense assignment. Here we have changed the sign of q_c for PNIC solutions.

(47) Green, M. M.; Zanella, S.; Gu, H.; Sato, T.; Gottarelli, G.; Jha, S. K.; Spada, G. P.; Schoevaars, A.-M.; Feringa, B.; Teramoto, A., in preparation.
(48) Lifson, S.; Felder, C. E.; Green, M. M. *Macromolecules* **1992**, *25*, 4142.
(49) Gottarelli, G.; Spada, G. P.; Garbesi, A. In *Comprehensive Supramolecular Chemistry*; Lehn, J.-M., Ed.; Pergamon: Oxford, 1996; Vol. 9, p 483.

MA970968O